Results in Physics 10 (2018) 264–269

Contents lists available at ScienceDirect

Results in Physics

journal homepage: www.elsevier.com/locate/rinp

Copper oxide nanomaterial saturable absorber as a new passive Q-switcher in erbium-doped fiber laser ring cavity configuration

Sinan Abdulhameed Sadeq[a,b,*], Sarah Kadhim Al-Hayali[a,b], Sulaiman Wadi Harun[c], Abdulhadi Al-Janabi[a]

[a] Institute of Laser for Postgraduate Studies, University of Baghdad, Baghdad, Iraq
[b] Al-Ma'moun University College, Baghdad, Iraq
[c] Department of Electrical Engineering, University of Malaya, Kuala Lumpur 50603, Malaysia

ARTICLE INFO

Keywords:
Q-switched
Erbium doped fiber
Passive
CuO
Saturable absorber

ABSTRACT

A passively Q-switched erbium-doped fiber laser (EDFL) operating at 1560 nm is demonstrated by using a copper oxide (CuO) film as a saturable absorber (SA). The SA was prepared by embedding CuO nanoparticles (NPs) into a polyvinyl alcohol (PVA) by solution casting method. The CuO-SA has a modulation depth of 3.5% and a saturation intensity of 3.3 MW/cm^2. By incorporating the CuO-SA into the laser cavity, stable Q-switched pulses were achieved at pump threshold of 70 mW. A maximum pulse energy of 66 nJ, tunable pulse repetition rate (P.R.R.) from 69 to 83 kHz, with a shortest pulse width of 2.6 μs were recorded at pump power of 159 mW. To the best of author's knowledge, this is the first demonstration of passively Q-switched EDFL based on CuO-SA.

Introduction

Short pulse fiber lasers found potential applications in many areas of photonics. Compared with continuous wave (CW) fiber laser, pulsed fiber lasers have the advantage of producing extremely high peak powers from short pulses, which are highly valuable for the applications such as nonlinear optics, medical treatment, range finding, fiber optic sensing and laser machining [1,2]. Those short pulses could be generated from CW or high repetition rate lasers using either Q-switching or mode locking mechanisms [2]. Basically, Q-switched pulse operation can be achieved by modulating the intra-cavity losses via active [3] or passive [4] techniques. In actively Q-switching fiber laser, an active (external) modulators, such as acousto-optic modulators (AOMs) [5,6] or electro-optic modulators (EOMs) [7] are essential to induce loss modulation. In contrast to active Q-switching, passive Q-switching based on SAs as a passive (internal) loss modulator has a significant advantages of compactness, low development costs and ease of integration into fiber laser cavity [8]. Throughout the past decades, various types of SAs have been tested and demonstrated as a successful Q-switch material, e.g., semiconductor saturable absorber mirrors (SESAMs) [9], nonlinear polarization rotation (NPR) [10], and nanomaterial with saturable absorption. Many kinds of nanomaterial SAs have been investigated to generate Q-switched pulses from EDFL, like, graphene [11], carbon nanotubes [12], gold nanorods [13], topological insulators (TIs) [14,15], hybrid SAs [16] and transition metal oxides (TMOs). TMO nanomaterials, show great advantages due to their wide absorption band, large nonlinearity, high optical damage threshold and fast recovery time [17]. ZnO [18,19], Fe_3O_4 [20,21], NiO [22], TiO_2 [17,23] and recently Al_2O_3 [24] have been fabricated and investigated as a compatible SAs. Wu et al. [25] have utilized a copper-nanowire as a saturable absorber in an EDFL linear cavity configuration to produce short pulses in the red (visible) region. The achieved result by Muhammed et al. [26] was 4.28 μs pulse duration using a pure copper nanoparticle as a SA in a ring cavity configuration of EDFL. Among various transition metal oxides, CuO presents itself as one of the promising material because of its wide range of applications in gas sensor [27], solar cell [28], field emitters [29], photovoltaic devices [30], and optical switches [31]. CuO NPs show remarkable and interesting physical and optical properties, including superconductivity at high temperature, non-toxicity, fast recovery time in range of picosecond and high third order nonlinearity[32]. Compared with some other TMOs (like ZnO [18], Al_2O_3 [24] and TiO_2 [17], CuO NPs has smaller bandgap of 1.2 eV [33] makes it more suitable in broadband saturable absorption for near IR pulsed laser system. According to its broadband operating bandwidth CuO-SA can act as an effective saturable absorber for Yb-doped fiber laser (1.06 μm). Different methods for fabricating CuO NPs as a thin film have been proposed [33,34]. In 2015 Rao et al. [35] used casting method to prepare polyving1 alcohol (PVA)-CuO nanocomposites with varying weight percentage of CuO NPs. PVA has been employed as a host matrix for incorporating CuO NPs due to its

* Corresponding author at: Institute of Laser for Postgraduate Studies, University of Baghdad, Baghdad, Iraq.
E-mail addresses: eng.sinan@ieee.org (S.A. Sadeq), swharun@um.edu.my (S.W. Harun), hadi.janabi@ilps.uobaghdad.edu.iq (A. Al-Janabi).

https://doi.org/10.1016/j.rinp.2018.06.006
Received 23 April 2018; Received in revised form 2 June 2018; Accepted 3 June 2018
Available online 06 June 2018

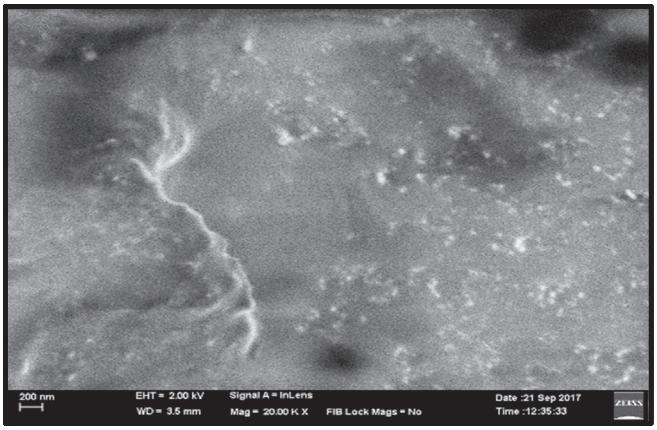

Fig. 1. FESEM image of CuO-SA NPs.

water solubility, transparently, non-toxicity and high durability [36]. Usually, thin film SAs are incorporated inside laser cavity either by dropping the SAs suspension directly on the end face ferrule of FC fiber connectors and letting it dry or by sandwiching the thin film between two FC fiber connectors via FC/PC fiber adapter [12].

In this work, we proposed and demonstrate passively Q-switched EDFL based on CuO-PVA thin film as a SA. The CuO-PVA thin film was prepared using casting technique [35]. By sandwiching CuO-PVA film between two FC/PC fiber connectors, stable Q-switched pulses were obtained at central wavelength of 1560 nm. The proposed CuO-SA is much easier to synthesize and simply integrated into all fiber ring cavity. CuO-PVA film is demonstrated experimentally for the first time as a new SA for passively Q-switched EDFL lasers.

Fabrication and characterization of a CuO based SA

In this experiment, CuO NPs (Skyspring nanomaterials) with particle size of ~40 nm and purity of 99% were used. The behavior of the CuO NPs as a SA can be improved by solving them with a polymer in form of thin film. The CuO-PVA nanocomposites were prepared using casting method. The thin film was obtained by adding the CuO into PVA. Firstly, the PVA host was prepared by blending 1 g of PVA powder in 100 ml of deionized water using magnetic stirrer for about 240 min up to the PVA powder was dispersed and solvent become homogenous. Then, 0.005 g of CuO NPs were added to PVA solution and stirred for 120 min. The resulting CuO-PVA nanocomposite was poured into well covered petri dishes and left in room temperature for 96 h. The thickness of prepared SA was about 2 μm. Fig. 1 shows the field emission scanning electron microscopy (FESEM) image of CuO-SA NPs, which approved the homogeneous distribution of SA and absence of aggregates.

Fig. 2 shows the Fourier transform infrared spectroscopy (FTIR) spectra for pure PVA (Fig. 2(a)) and CuO NPs (Fig. 2(b)). The FTIR spectrum of pure PVA shows that the PVA has peaks at 3383.14, 1737.86 and 1500 cm^{-1} verifying the O—H bond, C—O stretching bond and C—C bonding, respectively [24,30]. Fig. 2 (b) depicts the FTIR spectrum of pure CuO NPs and details the assignment of the corresponding peaks. The absorption peaks from 4000 to 500 cm^{-1} belong to the CuO. In particular, the vibrational peaks at 3469 cm^{-1} and 2925 cm^{-1} are due to the symmetric and asymmetric stretching vibration of O—H bond, respectively [37]. The absorption at 2350 cm^{-1} indicates the presence of atmospheric CO_2. The presence of bonds at 1038 cm^{-1} and 545 cm^{-1} represents different modes of bending vibration of Cu—O bond [37,38].

The nonlinear absorption of the CuO-SA was measured using stable short pulses 1.7 ps and P.R.R. 983 kHz with 1560 nm wavelength based on two detectors balanced technique. The fitting curve was drawn according to a simple two-level SA model [39]:

$$\alpha(I) = \frac{\alpha_s}{1 + I/I_{sat}} + \alpha_{ns}$$

where I is the input intensity, I_{sat} is the saturation intensity, α_s and α_{ns} are the modulation depth and non-saturable absorption respectively. Fig. 3(a) shows the resultant absorption measurement output as a function of intensity. The SA has a modulation depth of 3.5%, non-saturable absorption of 3.7% and saturation intensity of 3.3 MW/cm^2.

For the linear absorption characterization, an amplified spontaneous emission (ASE) source (Thorlabs SLD1550s-A1) operating from 1500 to 1600 nm has been used to illuminate the CuO-based SA. Fig. 3(b) shows that the operating region of the proposed Q-switched laser was between 1555 and 1565 nm, and centered at 1560 nm (highlighted by orange color) with insertion loss closed to -15.6 dB.

Experimental work

The setup of the Q-switched laser combined with CuO-based SA is shown in Fig. 4. The experimental setup consists of a 200 cm length of EDF as an active gain medium. It has a 23 dB/m peak absorption at

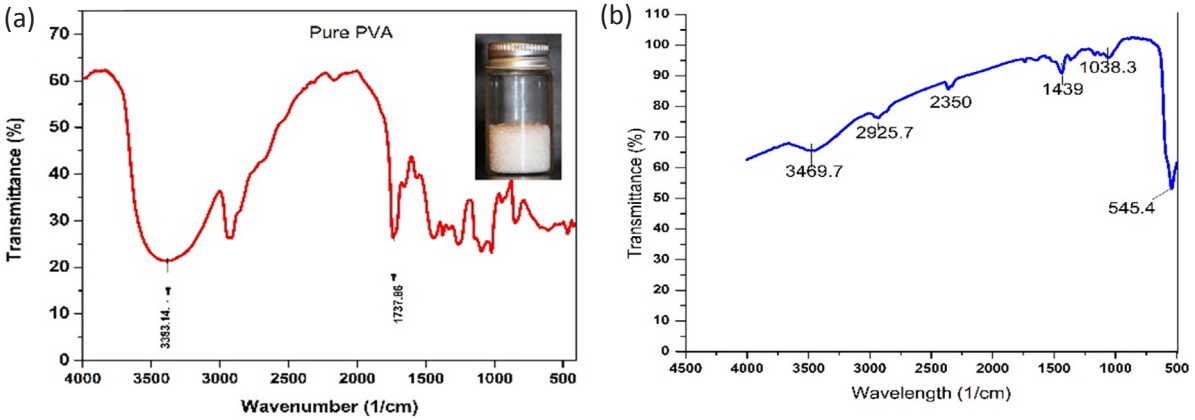

Fig. 2. FTIR spectra: (a) pure PVA and (b) CuO NPs.

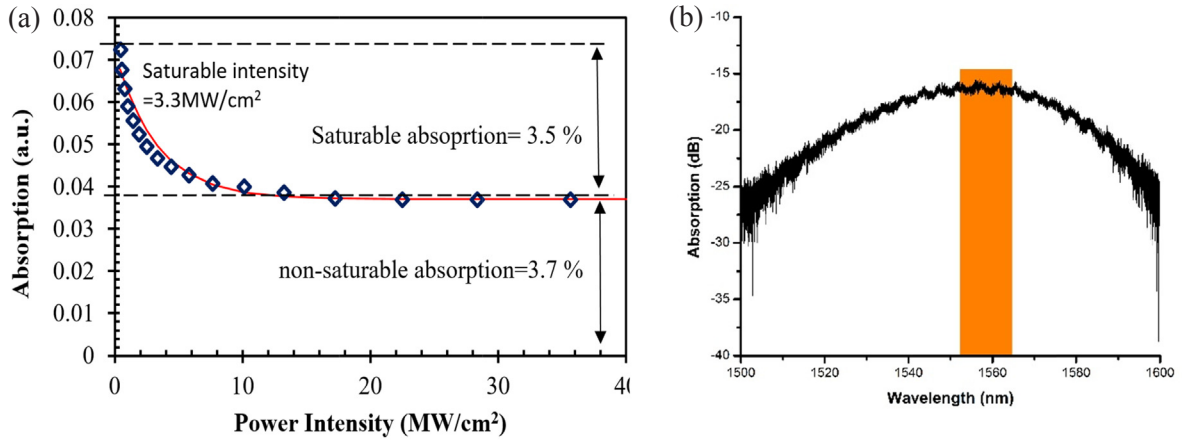

Fig. 3. (a) Nonlinear absorption curve of CuO (b) Linear absorption from 1500 to 1600 nm with lasing operation highlighted.

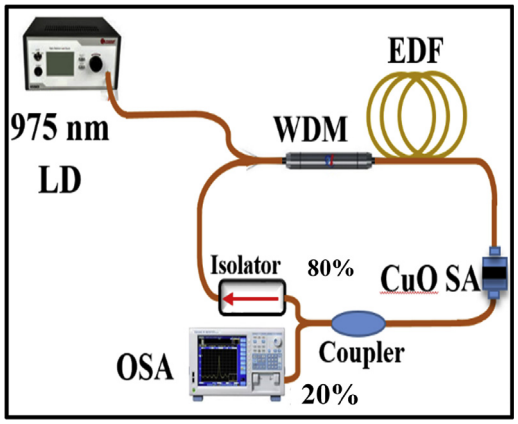

Fig. 4. Setup of passively Q-switched fiber laser based on CuO-SA.

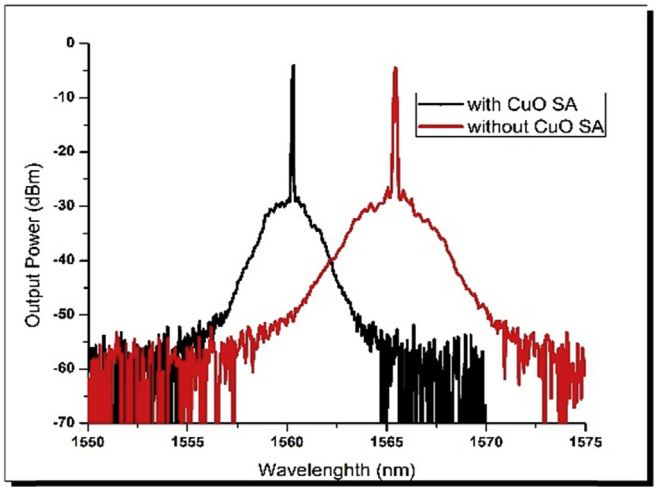

Fig. 5. Measured output laser spectrum of Q-switched EDFL: with and without CuO SA.

980 nm, core numerical aperture (NA) of 0.16 and 4 μm mode field diameter at 1550 nm. The EDF was excited by a 975 nm fiber coupled laser diode (LD) with maximum output power 159 mW via 980/1550 nm wavelength division multiplexer (WDM). One end of EDF was fusion spliced to the output port of the WDM, while the other end was connected to the input port of 20:80 fiber output coupler. 20% of the intra cavity power was extracted as an output via 20% arm of fiber coupler. An optical isolator (ISO) was employed to preserve unidirectional light propagation. The total cavity length was 7 m. The prepared thin film was incorporated into laser ring cavity by sandwiching a piece of 1x 1 mm from CuO-PVA thin film between two FC fiber connectors using gel matching index. In order to minimize the scattering losses within the light entering through varies refractive indices, an index matching gel with refractive index of 1.438 was used. The insertion loss for the SA has been measured −15.6 dB. The output information of the Q-switched laser were measured by GW INSTEK Oscilloscope (GDS-3352) combined with a 5 GHz InGaAs FC/PC fiber coupled photo-detector (Thorlabs) and optical power meter.

Results and discussion

At low pump threshold of 10 mW, CW operation of the proposed EDFL was firstly observed. By inserting CuO-PVA thin film into the ring cavity, passively Q-switched pulses are self-started at 70 mW input pump threshold and monitored on oscilloscope. Compared with recently published work [40], the threshold pump power value of this laser is relatively low. The output spectrum of the Q-switched laser was monitored by Anritsu (MS9710B) optical spectrum analyzer (OSA) which has resolution about 0.07 nm. The 3-dB bandwidth of the lasing wavelength spectrum was measured without and with SA thin film to be about 0.18 nm at the central wavelength of 1564 nm (red color) and 0.16 nm at the central wavelength of 1560 nm (black color), respectively as depicted in Fig. 5. The central wavelength was blue shifted around 4 nm when the CuO-SA incorporated inside the ring cavity due to the high loss of SA.

By boosting the pump source from threshold value of 70 mW to a maximum allowable power of 159 mW, a stable Q-switching pulses with 4.8–2.6 μs pulse width and 69–83 kHz repetition rate were observed. The output pulse train at different pump powers are summarized in Fig. 6.

Fig. 7 presents the symmetrical Gaussian profile of the shortest pulse width (2.6 μs). The measured pulsed width and repetition rate as a function of pump power is depicted in Fig. 8. It is clear that when the pump power increases, the gain will saturate the SA faster. This will lead to more pulse generation and consequently an increase in the

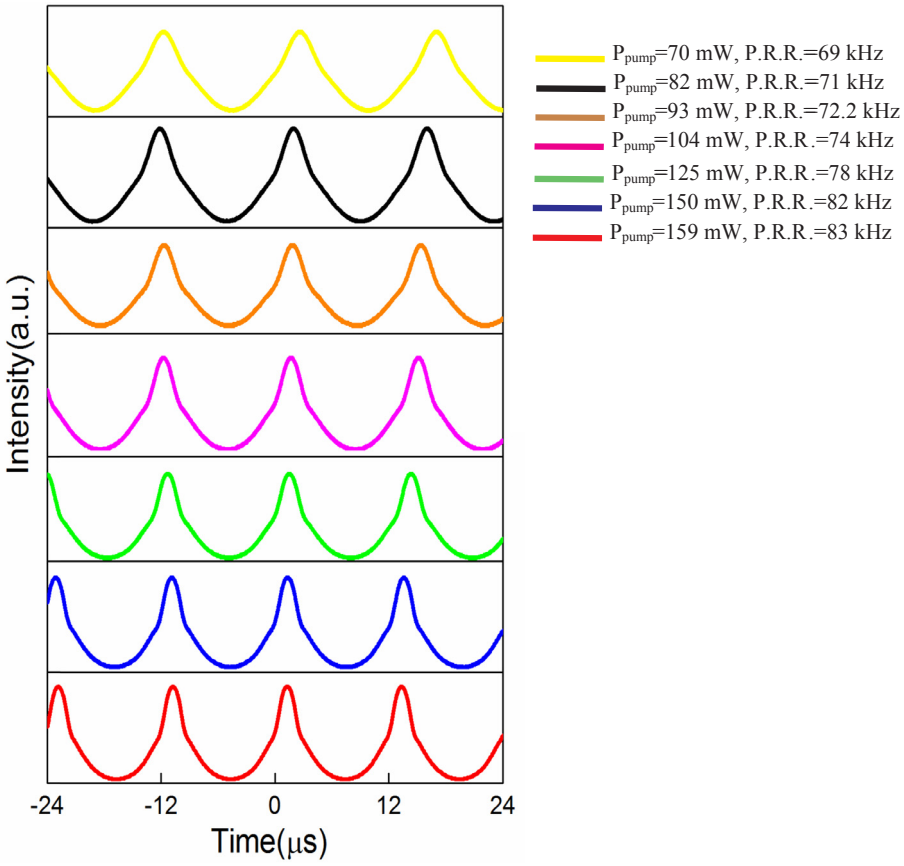

Fig. 6. Optical pulse train corresponding to the pumping threshold of 70 mW to maximum power of 159 mW.

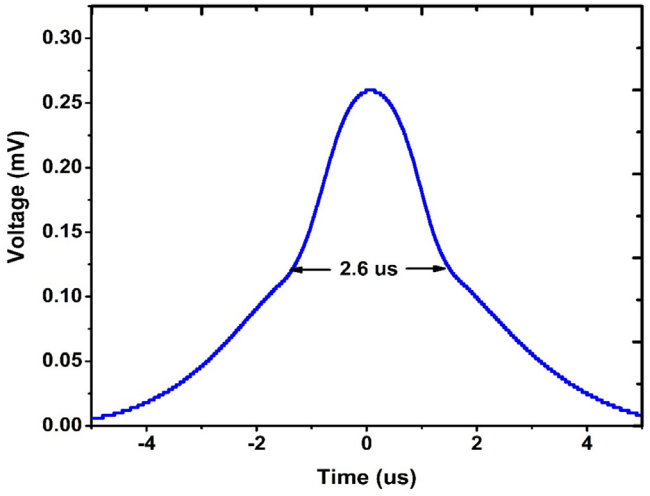

Fig. 7. A typical pulse profile of 2.6 μs at maximum pump power of 159 mW.

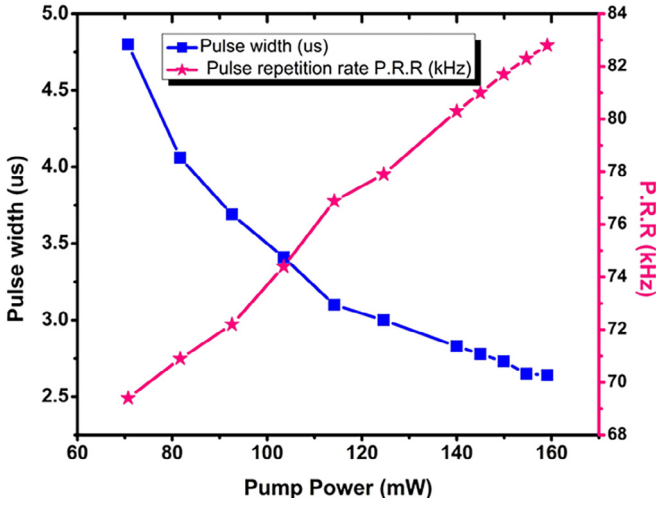

Fig. 8. Pulse repetition rate and pulse width as a function of pump power.

repetition rate while the pulse width decreases [41].

The calculated pulse energy and the measured output power versus the input pump power is depicted in Fig. 9. From this figure, the variation of the pulse energy (29–66) nJ as a function of the input pump power (70–159) mW has a linear relationship reflecting the typical performance of passively Q-switched fiber laser [42].

The laser stability was investigated by analyzing the radio frequency (RF) spectrum as shown in Fig. 10. The fundamental frequency of the output laser is obtained at 83 kHz with high signal to noise ratio (SNR) of about 59.5 dB. The resolution bandwidth (RBW) of RF was 3 kHz. This RF spectrum clearly indicates that the generated Q-switched pulses are stable over a wider span of 900 kHz. While the long term power stability of laser operation was investigated by monitoring the OSA spectrum for laser output over 1 h at intervals of 10 min as shown in

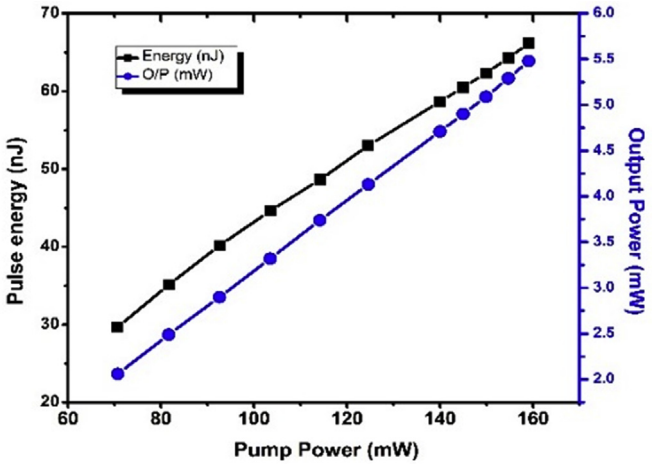

Fig. 9. The output power and pulse energy as a function of pump power.

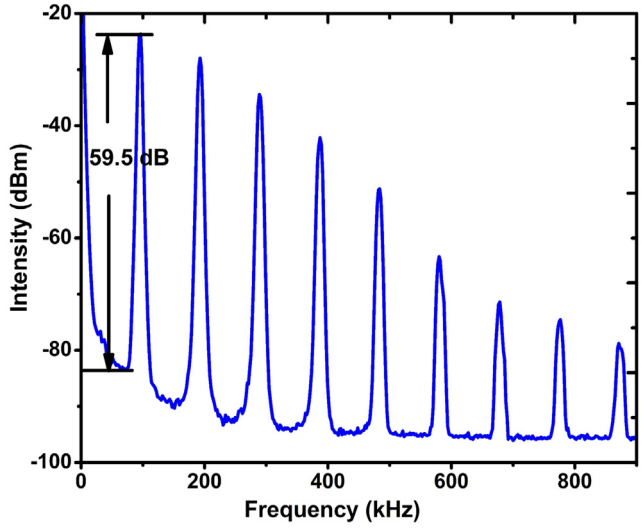

Fig. 10. RF spectrum at 159 mW of 83 kHz Repetition rate.

Fig. 11. Throughout the experimental work, by removing the CuO-SA from the cavity, CW operation is restored on oscilloscope, verifying that CuO-SA was the only modulator for achieving Q-switch operation with this setup.

Finally, the performance of the proposed Q-switched EDFL based on CuO-SA was compared with recently published Q-switched EDFL using

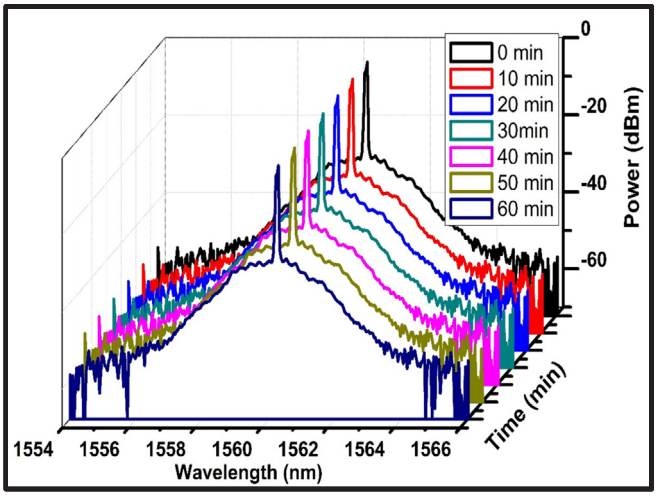

Fig. 11. Laser spectrum performance over 1 h.

other types of SAs materials such as Graphene, WSSe, Fe_3O_4, NiO, Al_2O_3, Cu and DWCNTs as listed in Table 1. Those results highlight that the demonstrated Q-switched laser based on CuO-SA has minimum pulse width. The P.R.R. and SNR are relatively high compared with the others. The maximum pulse energy and the pump threshold are comparable with other reported values. We can conclude that CuO-SA not inferior compared with other SAs.

Conclusions

We experimentally demonstrated passively Q-switched EDFL by utilizing the CuO-NPs based SA. CuO-SA acts as an intracavity modulation loss and used to achieve Q-switching operation at 1560 nm. As the pump power increases from 70 mW to 159 mW, the shortest pulse width of 2.6 μs, with the maximum pulse energy of 66 nJ and P.R.R. of 83 kHz were obtained. The experimental results show that CuO thin film is appropriate SA for short pulse generation. Therefore, EDFL based on CuO-SA is a promising in the ultra-fast photonics applications within C-band region due to its characteristics of low pulse width and high stability.

Funding

This work was partially funded by Institute of Laser for Postgraduate Studies at University of Baghdad in Iraq and the Ministry of Higher Education and Scientific Research in Iraq.

Table 1
Comparison between different types of thin film based SAs of Q-switched EDFL.

SA Material	Operating Wavelength (nm)	Minimum Pulse (μs)	Repetition Rate (kHz)	Pulse Energy (nJ)	Pump Threshold (mW)	SNR (dB)	Ref.	Year
Graphene	1558.28	6.02	67.8	206	51.6	62	[43]	2018
WSSe	1568.4	2.6	61.8	7.31	89	57.8	[44]	2018
Fe_3O_4-PVA	1557	6	28	71	25	–	[20]	2017
NiO	1561.2	5.2	52.18	31.5	25	55	[22]	2017
Al_2O_3	1560.6	2.8	81	56.7	158	56	[24]	2017
Cu	1561	4.28	101	18.2	26.1	50.9	[26]	2017
DWCNTs	1568.6	4.6	47	102.1	40	–	[12]	2016
CuO	1560	2.6	83	66	70	59.5	This work	

Acknowledgments

One of the authors, S.A. Sadeq would like to thank I.A.M. Alani and M.H.M. Ahmed (Department of Electrical Engineering, University of Malaya) for their valuable comments and help during the experimental demonstration.

References

[1] Tsai T-Y, Fang Y-C. A saturable absorber Q-switched all-fiber ring laser. Opt Express 2009;17(3):1429–34.
[2] Gattass RR, Mazur E. Femtosecond laser micromachining in transparent materials. Nat Photonics 2008;2(4):219–25.
[3] Cowle GJ, Stepanov DY. Multiple wavelength generation with Brillouin/erbium fiber lasers. IEEE Photonics Technol Lett 1996;8(11):1465–7.
[4] Paschotta R, et al. Passively Q-switched 0.1-mJ fiber laser system at 1.53 um. Opt Lett 1999;24(6):388–90.
[5] Kir'yanov AV, Barmenkov YO, Andres MV. An experimental analysis of self-Q-switching via stimulated Brillouin scattering in an ytterbium doped fiber laser. Laser Phys Lett 2013;10(5):055112.
[6] Villegas I, et al. Yb-doped strictly all-fiber laser actively Q-switched by intermodal acousto-optic modulation. Laser Phys 2011;21(9):1650.
[7] Bouyge D, et al. Synchronized tunable q-switched fiber lasers using deformable achromatic microelectromechanical mirror. IEEE Photonics Technol Lett 2008;20(12):991–3.
[8] Pan L, Utkin I, Fedosejevs R. Passively Q-switched ytterbium-doped double-clad fiber laser with a Cr4+:YAG saturable absorber. IEEE Photonics Technol Lett 2007;19(24):1979–81.
[9] Keller U, et al. Semiconductor saturable absorber mirrors (SESAM's) for femtosecond to nanosecond pulse generation in solid-state lasers. IEEE J Sel Topics Quantum Electron 1996;2(3):435–53.
[10] Komarov A, Leblond H, Sanchez F. Theoretical analysis of the operating regime of a passively-mode-locked fiber laser through nonlinear polarization rotation. Phys Rev A 2005;72(6):063811.
[11] Lin Y-H, et al. Using graphene nano-particle embedded in photonic crystal fiber for evanescent wave mode-locking of fiber laser. Opt Express 2013;21(14):16763–76.
[12] Mohammed D, Al-Janabi A. Passively Q-switched erbium doped fiber laser based on double walled carbon nanotubes-polyvinyl alcohol saturable absorber. Laser Phys 2016;26(11):115108.
[13] Fan D, et al. Passively Q-switched erbium-doped fiber laser using evanescent field interaction with gold-nanosphere based saturable absorber. Opt Express 2014;22(15):18537–42.
[14] Lu S, et al. Third order nonlinear optical property of Bi2Se3. Opt Express 2013;21(2):2072–82.
[15] Bonaccorso F, Sun Z. Solution processing of graphene, topological insulators and other 2d crystals for ultrafast photonics. Opt Mater Express 2014;4(1):63–78.
[16] Lin K-H, et al. Manipulation of operation states by polarization control in an erbium-doped fiber laser with a hybrid saturable absorber. Opt Express 2009;17(6):4806–14.
[17] Ahmad H, et al. C-band Q-switched fiber laser using titanium dioxide (TiO 2) as saturable absorber. IEEE Photonics J 2016;8(1):1–7.
[18] Ahmad H, et al. Zinc oxide (ZnO) nanoparticles as saturable absorber in passively Q-switched fiber laser. Opt Commun 2016;381:72–6.
[19] Ahmad H, et al. Q-switched ytterbium-doped fiber laser with zinc oxide based saturable absorber. Laser Phys 2016;26(11):115107.
[20] Mao D, et al. Q-switched fiber laser based on saturable absorption of ferroferric-oxide nanoparticles. Photonics Res 2017;5(1):52–6.
[21] Mohammed D, Khaleel WA, Al-Janabi A. Tunable Q-switched erbium doped fiber laser based on metal transition oxide saturable absorber and refractive index characteristic of multimode interference effects. Opt Laser Technol 2017;97:106–10.
[22] Nady A, et al. Nickel oxide nanoparticles as a saturable absorber for an all-fiber passively Q-switched erbium-doped fiber laser. Laser Phys 2017;27(6):065105.
[23] Rusdi MFM, et al. Titanium Dioxide (TiO 2) film as a new saturable absorber for generating mode-locked Thulium-Holmium doped all-fiber laser. Opt Laser Technol 2017;89:16–20.
[24] Al-Hayali SKM, et al. Aluminum oxide nanoparticles as saturable absorber for C-band passively Q-switched fiber laser. Appl Opt 2017;56(16):4720–6.
[25] Wu D, et al. Saturable absorption of copper nanowires in visible regions for short-pulse generation. IEEE Photonics J 2016;8(4):1–7.
[26] Muhammad A, et al. Q-switching pulse operation in 1.5-μm region using copper nanoparticles as saturable absorber. Chin Phys Lett 2017;34(3):034205.
[27] Yadav, VS, et al. The effect of frequency and temperature on dielectric properties of pure poly vinylidene fluoride (PVDF) thin films. In: Proceedings of the international multiconference of engineers and computer scientists. 2010.
[28] Zhang H, Zhang M. Synthesis of CuO nanocrystalline and their application as electrode materials for capacitors. Mater Chem Phys 2008;108(2):184–7.
[29] Shang D, et al. Magnetic and field emission properties of straw-like CuO nanostructures. Appl Surf Sci 2009;255(7):4093–6.
[30] Ray SC. Preparation of copper oxide thin film by the sol–gel-like dip technique and study of their structural and optical properties. Solar energy Mater Solar cells 2001;68(3):307–12.
[31] Xu Y, Chen D, Jiao X. Fabrication of CuO pricky microspheres with tunable size by a simple solution route. J Phys Chem B 2005;109(28):13561–6.
[32] Born B, et al. Ultrafast charge-carrier dynamics of copper oxide nanocrystals. ACS Photonics 2016;3(12):2475–81.
[33] Abaker M, et al. Structural and optical properties of CuO layered hexagonal discs synthesized by a low-temperature hydrothermal process. J Phys D Appl Phys 2011;44(15):155405.
[34] Shahmiri M, et al. Third-order nonlinear optical properties of chemically synthesized copper oxide nanosheets. Phys E: Low-dimensional Syst Nanostruct 2013;54:109–14.
[35] Rao JK, et al. Investigation of structural and electrical properties of novel CuO–PVA nanocomposite films. J Mater Sci 2015;50(21):7064–74.
[36] Kokabi M, Sirousazar M, Hassan ZM. PVA–clay nanocomposite hydrogels for wound dressing. Eur Polym J 2007;43(3):773–81.
[37] Raul PK, et al. CuO nanorods: a potential and efficient adsorbent in water purification. RSC Adv 2014;4(76):40580–7.
[38] Arun K, et al. Surfactant free hydrothermal synthesis of copper oxide nanoparticles. Am J Mater Sci 2015;5(3A):36–8.
[39] Garmire E. Resonant optical nonlinearities in semiconductors. IEEE J Sel Top Quantum Electron 2000;6(6):1094–110.
[40] Ahmad H, Tiu ZC, Ooi SI. Passive Q-switching in an erbium-doped fiber laser using tungsten sulphoselenide as a saturable absorber (Chinese Title: Passive Q-switching in an erbium-doped fiber laser using tungsten sulphoselenide as a saturable absorber). Chin Opt Lett 2018;16(2):020009.
[41] Degnan JJ. Optimization of passively Q-switched lasers. IEEE J Quantum Electron 1995;31(11):1890–901.
[42] Svelto O. Properties of laser beams, in principles of lasers. Springer; 2010. p. 475–504.
[43] Zuikafly SNF, et al. Conductive graphene as passive saturable absorber with high instantaneous peak power and pulse energy in Q-switched regime. Results Phys 2018;9:371–5.
[44] Ahmad H, Tiu Z, Ooi S. Passive Q-switching in an erbium-doped fiber laser using tungsten sulphoselenide as a saturable absorber. Chin Opt Lett 2018;16(2):020009.